Ecosystems (2021) 24: 699–712
https://doi.org/10.1007/s10021-020-00544-1

ECOSYSTEMS

Forest Structural Complexity and Biomass Predict First-Year Carbon Cycling Responses to Disturbance

Christopher M. Gough,[1]* Jeff W. Atkins,[1] Ben Bond-Lamberty,[2] Elizabeth A. Agee,[3] Kalyn R. Dorheim,[2] Robert T. Fahey,[4] Maxim S. Grigri,[1] Lisa T. Haber,[1] Kayla C. Mathes,[1] Stephanie C. Pennington,[2] Alexey N. Shiklomanov,[5] and Jason M. Tallant[6]

[1]*Department of Biology, Virginia Commonwealth University, 1000 West Cary St., Box 842012, Richmond, Virginia 23284, USA;* [2]*Joint Global Change Research Institute, Pacific Northwest National Laboratory, 5825 University Research Ct, College Park, Maryland 20740, USA;* [3]*Environmental Sciences Division, Climate Change Science Institute, Oak Ridge National Laboratory, Oak Ridge, Tennessee 37831, USA;* [4]*Department of Natural Resources and the Environment, Center for Environmental Sciences and Engineering, University of Connecticut, 1376 Storrs Road, Storrs, Connecticut 06269, USA;* [5]*NASA Goddard Space Flight Center, Greenbelt, Maryland 20771, USA;* [6]*Biological Station, University of Michigan, Pellston, Michigan 49769, USA*

ABSTRACT

The pre-disturbance vegetation characteristics that predict carbon (C) cycling responses to disturbance are not well known. To address this gap, we initiated the Forest Resilience Threshold Experiment, a manipulative study in which more than 3600 trees were stem girdled to achieve replicated factorial combinations of four levels (control, 45, 65, and 85% gross defoliation) of disturbance severity and two disturbance types (targeting upper or lower canopy strata). Applying a standardized stability framework in which initial C cycling resistance to disturbance was calculated as the first-year natural log response ratio of disturbance and control treatments, we investigated to what extent pre-disturbance levels of species diversity, aboveground woody biomass, leaf area index, and canopy rugosity—a measure of structural complexity—predict the initial responses of subcanopy light-saturated leaf CO_2 assimilation (A_{sat}), aboveground wood NPP ($ANPP_w$), and soil respiration (R_s) to phloem-disrupting disturbance. In the year following stem girdling, we found that aboveground C cycling processes, A_{sat} and $ANPP_w$, were highly resistant to increases in disturbance severity, while R_s resistance declined as severity increased. Disturbance type had no effect on first-year resistance. Pre-disturbance aboveground woody biomass, and canopy rugosity were positive predictors of $ANPP_w$ resistance and, conversely, negatively related to R_s resistance. Subcanopy A_{sat} resistance was not related to pre-disturbance vegetation characteristics. Stability of C uptake processes along with R_s declines suggest the net C sink was sustained in the initial months following disturbance. We conclude that biomass and complexity are significant, but not universal, predictors of initial C cycling resistance to disturbance. Moreover, our

Received 4 May 2020; accepted 1 August 2020;
published online 21 August 2020

Electronic supplementary material: The online version of this article (https://doi.org/10.1007/s10021-020-00544-1) contains supplementary material, which is available to authorized users.

Author contributions CMG and BBL conceived and designed the study; CMG, JWA, BBL, KRD, RTF, MSG, LTH, KCM, SCP, ANS, and JMT performed research and analyzed data; CMG led and all others contributed to the writing of the paper.

**Corresponding author; e-mail:* cmgough@vcu.edu

findings highlight the utility of standardized stability measures when comparing functional responses to disturbance.

Key words: disturbance; stability; resistance; carbon cycling; forests; production; soil respiration; photosynthesis; diversity; complexity; stem girdling.

HIGHLIGHTS

- The vegetation characteristics that support functional stability are largely unknown.
- Biomass and complexity predict first-year forest C cycling responses to disturbance.
- Greater pre-disturbance biomass and complexity sustained production but reduced soil respiration.

INTRODUCTION

The diversity, quantity, structure, and complexity of vegetation predict plant population and community stability following disturbance, but the vegetation characteristics that confer functional—including carbon (C) cycling—stability are poorly understood (Brockerhoff and others 2017; Hillebrand and Kunze 2020; Johnstone and others 2016). This lack of knowledge is particularly acute for forest ecosystems, with current understanding limited to the stabilizing effects of species diversity on gross and net primary production (Jucker and others 2014; Musavi and others 2017; Pedro and others 2015). The links between vegetation characteristics and C cycling stability have been investigated more thoroughly in easier-to-manipulate grasslands (Hillebrand and Kunze 2020), but forests and grasslands may respond differently to identical disturbances because plant adaptive strategies vary between woody and herbaceous plants (Stuart-Haentjens and others 2018). Consequently, inferring forest functional responses from grassland disturbance studies may lead to spurious ecological forecasts and the misguided management of C cycling stability.

Among the multiple dimensions of stability, *resistance* describes the initial community compositional or ecosystem functional response to disturbance (Figure 1). Functional resistance can be derived and interpreted using a multidimensional stability framework that quantitatively describes several stages of a disturbance and recovery cycle, where negative and positive values indicate a decline and increase, respectively, in functioning (Hillebrand and others 2018). This approach, rarely used to characterize the functional stability of forests, allows for standardized comparisons of stability among different ecological processes, ecosystem types, and disturbance severities and regimes (Hillebrand and Kunze 2020). In addition, initial resistance could foreshadow longer-term functional change, including resilience, temporal stability, and recovery (Radchuk and others 2019; Stuart-Haentjens and others 2018), thereby providing a potential ecological diagnostic of future stability.

Although functional resistance values are lacking for forests, prior observations suggest changes in the C cycle immediately following disturbance may be neutral, negative or, unlike immediate population and community responses, positive. For example, in temperate forests, subcanopy leaf net CO_2 assimilation (A) generally increases following the senescence of upper canopy trees, signifying positive, compensatory physiological resistance in the lower canopy strata that may stimulate the growth of seedlings and saplings (Fahey and others 2016; Stuart-Haentjens and others 2015). In contrast, temperate forest net primary production (NPP) and soil respiration (R_s) may increase, decrease, or remain the same, depending on the severity and the type of disturbance (Amiro and others 2010; Borkhuu and others 2015; Clark and others 2010; Gough and others 2013; Levy-Varon and others 2012). Pre-disturbance vegetation characteristics, such as diversity, biomass, leaf area index (LAI), and complexity are proposed, but have not been shown empirically, to influence the sign and magnitude of forest functional resistance (Hillebrand and Kunze 2020; Johnstone and others 2016). Moreover, the sensitivity of functional stability to vegetation characteristics is hypothesized to increase as severity increases, as ecological legacies are theorized to play a progressively essential role in the recovery of function to pre-disturbance levels (Johnstone and others 2016; Koontz and others 2020). Identifying which vegetation characteristics are associated with multi-process C cycling resistance will aid in sustaining the terrestrial C sink as disturbance regimes change (Liu and others 2019).

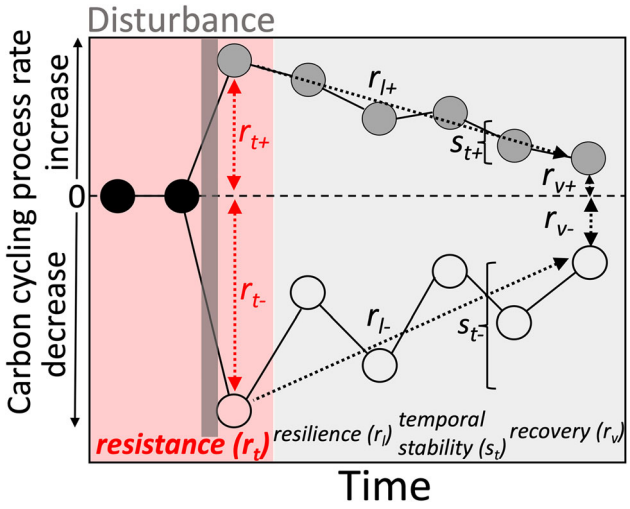

Figure 1. A conceptual illustration of the multidimensional stability framework summarized by Hillebrand and others (2018), modified to highlight potential changes in carbon (C) cycling process rate following disturbance (vertical dark gray bar). *Resistance* (r_t, red-shaded), our focus, is the initial response, estimated as the natural log ratio of the mean carbon flux/process rates following disturbance to that of a control or pre-disturbance value and can be positive or negative. Illustrated (gray-shaded), but not considered in our analysis of initial disturbance response, are: *resilience*, the carbon flux change (or slope) over time; *temporal stability*, the degree of variation over time in carbon flux calculated as the coefficient of variation in interannual mean C fluxes; and *recovery*, the final difference in carbon flux rate between disturbed and control or pre-disturbance baseline.

We implemented a large-scale, fully replicated forest disturbance experiment in which more than 3600 trees were stem girdled with a goal of identifying which pre-disturbance vegetation characteristics predict the response of C cycling processes to variable disturbance severity and different disturbance types. We define ''vegetation characteristics'' as plant community, stand or canopy features that might affect functional stability, focusing specifically on woody plant diversity, aboveground woody biomass, leaf area index (LAI) and canopy rugosity (that is, canopy structural complexity). Our research site has a common disturbance history of clear-cut harvesting and fire a century ago, and thus spatial variation in vegetation characteristics is a result of differences in soils, landform and plant community composition (Table 1, Lapin and Barnes 1995). Focusing on the first-year response to experimental phloem-disrupting disturbance, our specific objectives were to determine whether: 1) subcanopy light-saturated leaf A (A_{sat}), aboveground wood NPP ($ANPP_w$), and the soil-to-atmosphere CO_2 flux (soil respiration, R_s) exhibit similar resistance across variable levels of disturbance severity and in response to different disturbance types; 2) pre-disturbance vegetation characteristics affect subsequent C cycling resistance to disturbance; and 3) vegetation characteristics are stronger predictors of resistance at high disturbance severities.

METHODS

Study Site and Experiment

Our experiment was conducted at the University of Michigan Biological Station (UMBS) in northern lower Michigan, USA (45.56 N, − 84.67 W), where mean annual air temperature is 5.5°C and mean annual precipitation is 817 mm (Gough and others 2013). The vegetation communities included in our analysis are transitioning 100-year-old middle successional forests, with a dominant upper canopy comprised mainly of pioneer bigtooth and trembling aspen (*Populus grandidentata* and *P. tremuloides*, respectively) and paper birch (*Betula papyrifera*) established following region-wide harvesting and fire in the early twentieth century (Figure 2A). This cohort of early successional tree species is rapidly declining (Gough and others 2010), and giving way to later successional red oak (*Quercus rubra*), eastern white pine (*Pinus strobus*), sugar maple (*Acer saccharum*), red maple (*Acer rubrum*), and American beech (*Fagus grandifolia*). Despite sharing a relatively uniform disturbance history, tree species' dominance, and plant community composition along with structure and complexity vary substantially among the ''landscape ecosystems'' of UMBS (Table 1; Figure 2; Scheuermann and others 2018). The term ''landscape ecosystems'' is used to describe land units

Table 1. The Vegetation Characteristics, Landforms and Soil Textures of Treatment Replicates in the Forest Resilience Threshold Experiment (FoRTE) Before Disturbance Severity and Disturbance Type Treatments Were Implemented

	A	B	C	D
Canopy tree (> 8 cm D) composition	POGR (61%) ACSA (17%) ACRU (10%) FAGR (10%)	POGR(58%) ACRU (24%) QURU (9%) FAGR (4%)	QURU (43%) POGR (39%) PIST (6%) ACRU (6%)	QURU (72%) POGR (19%) PIST (4) FAGR (1%)
Stem density (stems ha^{-1}, > 8 cm D)	865 (32)[a]	888 (46)[a]	910 (55)[a]	796 (81)[a]
Shannon's index of species diversity	1.05 (0.09)[a]	1.05 (0.05)[a]	1.04 (0.11)[a]	0.92 (0.10)[a]
Leaf area index (dimensionless)	4.1 (0.15)[a]	3.6 (0.08)[b]	3.5 (0.10)[b]	2.9 (0.18)[c]
Biomass (kg C ha^{-1})	264,600 (15,800)[a]	229,900 (24,700)[ab]	197,000 (13,900)[ab]	155,900 (19,000)[c]
Canopy rugosity (m)	28.8 (3.6)[a]	22.3 (2.3)[b]	14.2 (1.7)[c]	8.9 (1.1)[d]
Landform	Moraine	Outwash over moraine	Outwash plain	Outwash plain
Soil texture	Sandy loam	Sand	Sand	Sand

Each color-coded and alphabetically assigned replicate is contained within a separate landscape ecosystem differentiated by vegetation and soils (see Figure 2A). Non-overlapping superscript letters indicate significant pairwise (least significant) differences among replicates ($P < 0.1$) of ≥ 204.2 stems ha^{-1} for stem density; 0.24 for Shannon's; 0.33 for leaf area index; 45,256 kg C ha^{-1} for biomass; and 1.72 m for canopy rugosity. Mean (± 1 S.E.), with the exception of canopy tree composition (% of total biomass)

forming a unique complex of climate, soils, biota and landform (Pearsall and others 1995). The compositional and structural variability associated with landscape ecosystems is paralleled by substantial spatial variability in NPP, which spanned a fourfold range across our site prior to experimental disturbance (Hardiman and others 2011).

We established the Forest Resilience Threshold Experiment (FoRTE) with the goal of understanding how and why disturbance severity and type affect key C cycling processes and ecosystem C balance. During Spring 2019, we randomly assigned factorial combinations of disturbance severity (4 levels) and type (2 levels) within four separate landscape ecosystems representing a range in site productivity characteristic of the forests of the Upper Great Lakes Region (Lapin and Barnes 1995). The approach used to implement disturbance was stem girdling, which, like wood-boring insects (for example, emerald ash borer, mountain pine beetle), causes gradual defoliation by eliminating the transport of photosynthate to roots, killing trees once carbohydrate reserves are exhausted over a period of 2 to 3 years (Dietze and others 2014; Gough and others 2013).

In late May 2019 (days 140–143), prior to leaf out, we selected more than 3600 trees for girdling from censused and mapped stems at least 8 cm diameter at breast height (DBH). Specifically, within each of the four replicates, we used species- and site- or region-specific allometries (Gough and others 2008) relating DBH to leaf area to target gross LAI reductions within each plot of 0% (control), 45, 65, or 85%. Severity levels were assigned at random to four, 0.5 ha circular whole plots, which were split into 0.25 ha halves and randomly designated a ''top-down'' or ''bottom-up'' disturbance type treatment (Figure 2B). For the ''top-down'' disturbance type, we girdled the largest trees first, irrespective of species, starting with the highest leaf area individual and sequentially girdling lower leaf area trees until the assigned plot disturbance severity was reached. For the ''bottom-up'' treatment, we stem girdled trees (> 8 cm DBH) with the lowest individual leaf area first, progressively girdling larger trees up to the targeted disturbance severity. Stem girdling was achieved through the chainsaw and pry bar facilitated removal of a 10-cm-wide circular band of phloem tissue (minimizing damage to the xylem) about 1 m above the forest floor and below DBH.

Circular, sampling subplots of 0.1 ha were established within each disturbance severity x type treatment in each of the four replicates, resulting in

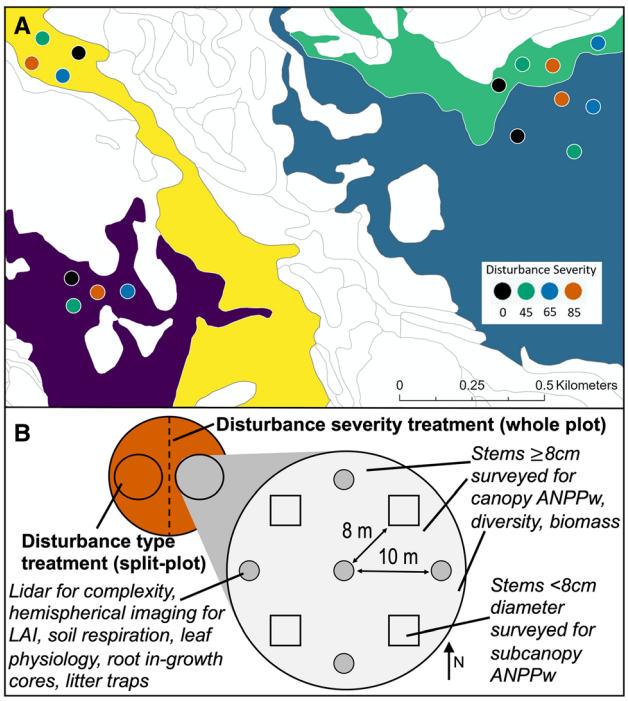

Figure 2. Forest Resilience Threshold Experiment (FoRTE) plot distribution map (**A**) and experimental design (**B**). Replicates of (0, 45, 65 or 85%) gross defoliation disturbance severities levels (map inset) and (top-down or bottom-up) disturbance types are distributed within four different landscape ecosystems spanning a significant gradient of leaf area index, woody plant biomass and canopy rugosity, as measure of canopy structural complexity (see Table 1). Multiple vegetation characteristics and carbon (C) cycling processes are characterized within each plot. The current analysis focuses on the resistance of three C cycling processes: subcanopy light-saturated leaf CO_2 assimilation rate (A_{sat}), aboveground wood net primary production ($ANPP_w$), and soil respiration (R_s).

a total of 32 subplots surrounded by at least a 5-m-wide measurement-free treatment buffer. Within each subplot and following methods detailed below, we measured $ANPP_w$, R_s, and A_{sat}, and we used terrestrial (that is, ground-based) lidar and hemispherical imagery along with stem census data to derive measures of diversity, structure and complexity. Because of variation among C cycling processes in sampling effort and timing, the frequency of measurements varied. Our methods are summarized below and described extensively in vignettes contained within the project's open field notebook: https://fortexperiment.github.io/fortedata/.

Light Saturated Leaf CO_2 Assimilation

Between July 8 and 28, 2019, we characterized the light-saturated CO_2 assimilation (A_{sat}) of leaves in the subcanopy of each subplot. Our A_{sat} measurements were broadly distributed to encompass the representative inter- and intra-specific physiological variation of each subplot, with three leaves 1–2 m above the forest floor randomly selected in each of four 2 m × 2 m sampling areas for a total of 12 leaves per subplot. When leaves in the 1–2 m stratum were not present, the closest seedling or sapling leaf outside of the sampling area was selected for measurement. We measured A_{sat} using an LI-6400 XT portable photosynthesis system (LI-COR Inc., Licoln, NE) programmed to maintain the following chamber conditions: 2000 μmol m^{-2} s^{-1} Photosynthetically Active Radiation (PAR), 400 ppm CO_2, 25°C air temperature and a vapor pressure deficit (VPD) target of less than 2 kPa. Leaves that failed to produce stable A_{sat} after 300 s were discarded and a new leaf from the same branch selected. The number of leaves measured across all 32 subplots totaled 391, including seven duplicates that were sampled when A_{sat} failed to stabilize. Mean resistance was inclusive of all species and, given our distributed sampling design, indicative of average subcanopy A_{sat}.

Aboveground Wood Net Primary Production

We calculated mean daily aboveground wood net primary production ($ANPP_w$) from repeated measurements of allometrically derived aboveground

wood mass. During summer 2018, we conducted a full census of trees with DBH at least 8 cm in all subplots, identifying each individual to the species level and measuring DBH using a tape. In the same year, we applied dendrometer bands to 23% (n = 666 total) of the total sampled population (n = 2903), selecting a subset of individuals within each subplot via the random stratification of species, DBH size classes, and girdled/non-girdled designation. In 2019, a single technician recorded the DBH of banded trees weekly on 15 separate dates from May through August, and twice during the dormant season in April and November. Smaller trees (1–8 cm DBH) were measured every other week from May through August in four 2 m × 2 m sampling areas using calipers; when no stems were present in these sampling areas, the two closest stems in the 1–8 cm size class were sampled for DBH. For trees less than 1 cm DBH, seedlings and saplings in a 1 m × 1 m quadrant of each vegetation sampling area were measured for base diameter and height using calipers and a measuring tape, respectively, in May and August 2019. For trees at least 1 cm DBH, species-, site-, or region-specific allometries were used to estimate aboveground wood mass from DBH on each sampling date (Gough and others 2008). Species- and DBH-specific relative growth rates (RGR) were generated from sampled stems and the daily wood production of unsampled trees was estimated as the product of subplot-, species-, and DBH-adjusted RGR and woody biomass. Total subplot $ANPP_w$ was the sum of individual-tree production scaled to the hectare and converted to C mass by multiplying each value by a site-specific C fraction of 0.48 (Gough and others 2008).

Soil Respiration

We repeatedly measured soil respiration from 160 soil collars in 2019. Each of the 32 subplots contained five, 10-cm-diameter PVC collars, and *in situ* point R_s measurements were made using a LI-6400 portable gas analyzer equipped with a LI-COR soil CO_2 chamber (LI-COR Inc, Lincoln, NE, USA). Two R_s values were recorded at each collar during separate 90-second intervals and averaged for analysis. All collars were sampled within a 2-day precipitation-free and weather-stable period 1 week before the experimental disturbance and a day after (mid-May), six times through the growing season (June–August), and once in late November.

Diversity, Structure and Complexity

We examined how initial C cycling responses were affected by four pre-disturbance (2018) vegetation characteristics with ties to ecosystem functioning: Shannon's Index of species diversity (or ''species diversity'' for brevity), leaf area index (LAI), aboveground wood biomass, and canopy rugosity. Following an experiment-wide 2018 census of 2903 stems with DBH, values of at least 8 cm, we estimated aboveground wood biomass for each subplot using species- and site- or region-specific equations following a standard protocol for our site (Gough and others 2008). Using stem inventory data, we also calculated stem basal area weighted Shannon's Index of species diversity via the *vegan* package version 2.5-6 (Legendre and others 2011) in R 3.6.2 (R Core Group, 2020). Subplot LAI was estimated optically using hemispherical imagery. We imaged the canopy in five, non-overlapping locations 1 m above the forest floor using a near-infrared (NIR) Sony Alpha 6000 24.3 Megapixel DSLR camera with a 180° hemispherical lens. Images were processed and LAI estimated using WinsCanopy software, which uses the NIR signal to distinguish green leaves from other tissues (Regent Instruments, Quebec, Qu) and produces LAI estimates that are highly correlated (r^2 = 0.87) with independently derived litter trap-based LAI values for our site (Stuart-Haentjens and others 2015). Lastly, we used terrestrial lidar to characterize subplot structural complexity as ''canopy rugosity'', which is broadly linked with processes such as NPP (Gough and others 2019; Hardiman and others 2011) and canopy light absorption (Atkins and others 2018b). A portable canopy lidar (PCL) system equipped with an upward facing, Riegl 3100VHS near-infrared pulsed-laser operating at 2000 Hz (Riegl LD90 3100 VHS; Riegl USA Inc., Orlando, Florida, USA) was used to create a hit grid of vegetation density along two 40 m (N–S, E–W) transects within each subplot (Hardiman and others 2013). Canopy rugosity was calculated using the *forestr* package version 1.0.1 (Atkins and others 2018a) in R.

Carbon Cycling Resistance Derivation

With the aim of deriving intercomparable measures of C cycling stability, we adopted the approach of Hillebrand and others (2018) to estimate the resistances of $ANPP_w$, A_{sat} and R_s to first-year disturbance (Figure 1). In this framework, *functional resistance* (r_t) is the natural log response ratio of

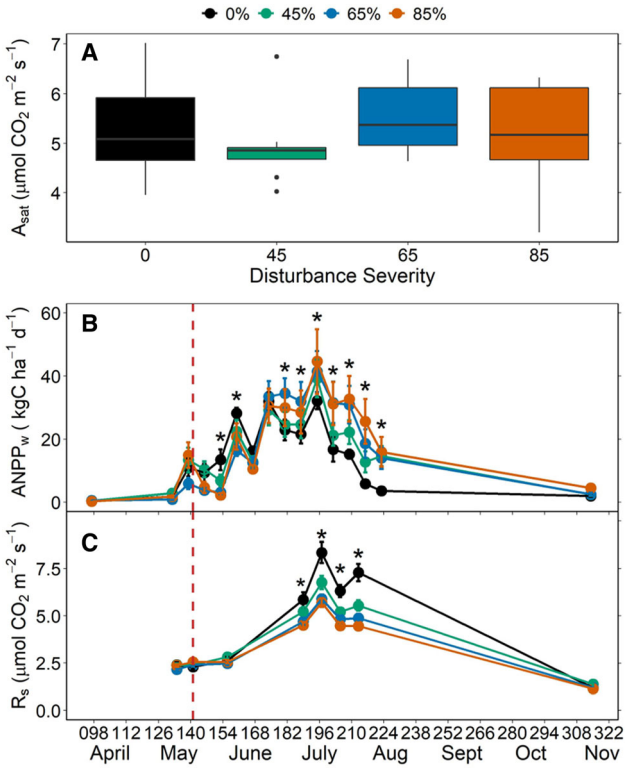

Figure 3. Mean subcanopy light-saturated leaf CO_2 assimilation rate (A_{sat}, **A**) and time-series of mean daily aboveground wood net primary production ($ANPP_w$, **B**) and soil respiration (R_s, **C**) by disturbance severity treatment, 2019. The vertical dashed line illustrates the time of stem girdling and asterisks convey significant ($P < 0.1$; least significant differences of 8.4 for $ANPP_w$ and 0.94 for R_s) within-date differences among disturbance severity treatments, with corresponding statistical parameters detailed in Table S1.

disturbed (F_{dist}) and control (F_{cont}) functioning–here, C cycling process rates:

$$r = \ln\left(\frac{F_{dist}}{F_{cont}}\right) \quad (1)$$

We derived r for A_{sat} ($r_{A_{sat}}$), $ANPP_w$ (r_{NPP}) and R_s (r_{R_s}) by dividing the respective subplot-level C cycling process means of each factorial combination of 45, 65, and 85% disturbance severity and top-down and bottom-up disturbance types A_{sat}, (F_{dist}) by mean control values (F_{cont}). For r_{NPP} and r_{R_s}, we calculated mean F_{dist} and F_{cont} from cumulative growing season $ANPP_w$ and annual R_s means (after disturbance), respectively, since data were collected on multiple dates, whereas $r_{A_{sat}}$, measured once, was derived from data collected during a single measurement campaign. In our study, resistance values that are less than 0 convey a decline in function (here, C cycling process rate), zero signals no change in function (that is, full resistance), and > 0 signifies an increase in function following disturbance relative to the control. In this initial analysis of disturbance effects, resistance values reflect only first-year C cycling responses to stem girdling disturbance treatments.

Statistical Analysis

The effects of disturbance type and severity on C cycling process rates and resistances were compared statistically using a modified split-plot mixed-effects ANOVA, in which disturbance severity was the fully randomized whole-plot and disturbance type was a restrictively randomized split-plot (Figure 2B). This model structure was applied to A_{sat}, $r_{A_{sat}}$, r_{NPP} and r_{R_s}, and included repeated measures (that is, with ''time'' as a separate variable) for $ANPP_w$ and R_s. Because their treatment assignment could not be fully randomized, the effects of disturbance type and time were tested using separate, more restrictive within-subject random effects error terms. Pair-wise post hoc comparisons of disturbance severity and time x disturbance severity used LSD, $\alpha = 0.1$, with the *a priori* expectation that C cycling rates and resistances would decline with

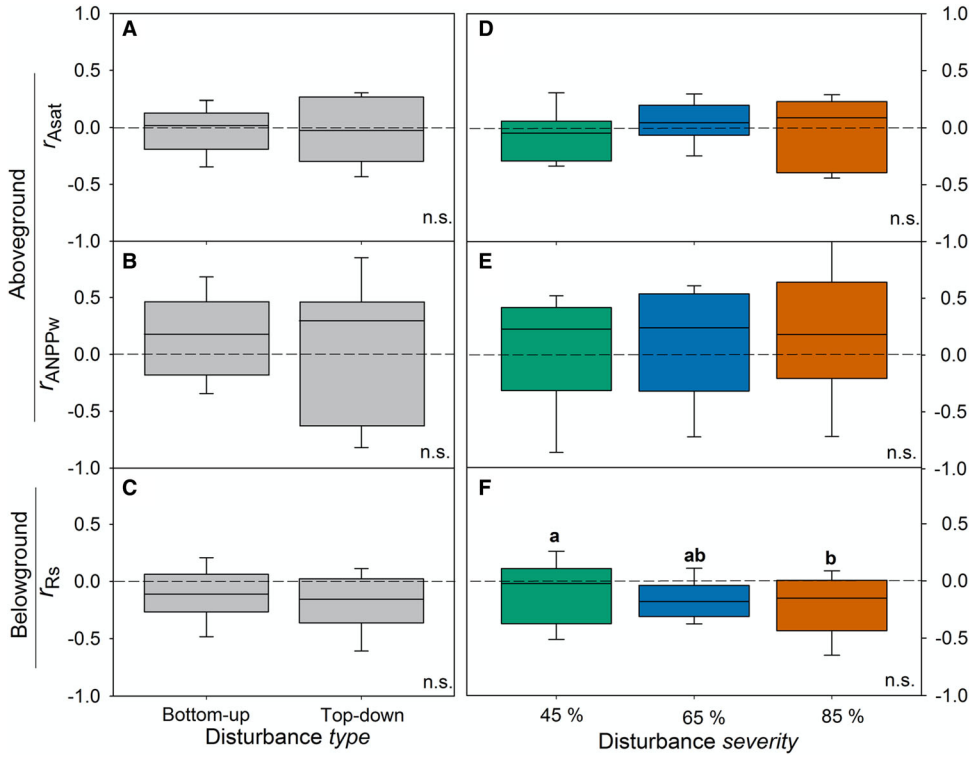

Figure 4. Box plot of median resistance values (middle horizontal line within box), interquartile ranges (box) and maximum and minimum values (whiskers) for subcanopy light-saturated leaf CO_2 assimilation rate ($r_{A_{sat}}$), net primary production (r_{NPP}) and soil respiration (r_{R_s}) by disturbance type (**A–C**) and disturbance severity (**D–F**). Above-ground carbon flux resistances, $r_{A_{sat}}$ and r_{NPP}, did not vary by disturbance type or severity; r_{R_s} declined with increasing disturbance severity but was unaffected by disturbance type. Non-overlapping letters in panel ''f'' denote significant pairwise (least significant) differences in mean r_{R_s} among disturbance severities ($P < 0.1$) of ≥ 0.11, with corresponding statistical parameters detailed in Table S2.

increasing disturbance severity. To evaluate whether pre-disturbance vegetation characteristics predict r_A, r_{NPP}, and r_{R_s}, we correlated plot-scale (that is, by averaging subplots) Shannon's Index of species diversity, woody plant biomass, LAI and canopy rugosity with resistance values. For concision, we focus our presentation on the effects of disturbance severity and not type, because only the former (presented in Figure 4) significantly affected C cycling processes. We first fit linear multivariate models containing disturbance severity, the vegetation characteristic of interest, and the statistical interaction between the two to $r_{A_{sat}}$, r_{NPP}, and r_{R_s}. If the main effect of the ecosystem property on resistance but not the interaction was significant ($P < 0.1$), we fit a single linear model to the data; however, if the interaction was significant, then separate linear models were fit to each disturbance severity when $P < 0.1$. For all C cycling variables, uncertainty was propagated analytically from sampling error and expressed as a standard error of the mean. We report correlations and pairwise comparisons when $P < 0.1$, while acknowledging that C cycling processes following disturbance are dynamic and subject to future change. The statistical models and parameters (specific P and F values, degrees of freedom) supporting our data figures are presented in Tables S1–3. Project data are supplied in near real-time through an open notebook (https://fortexperiment.github.io/fortedata/) and code associated with statistical analysis is available via https://doi.org/10.5281/zenodo.3779040.

RESULTS

First-Year Defoliation and Carbon Cycling Process Rates

Stem girdling had little effect on LAI in the first growing season. No declines in LAI between peak leaf out and prior to leaf drop were observed at any mean (cross-replicate) disturbance severity level or in either of the disturbance types. When changes in LAI during the leaf-on period were considered at

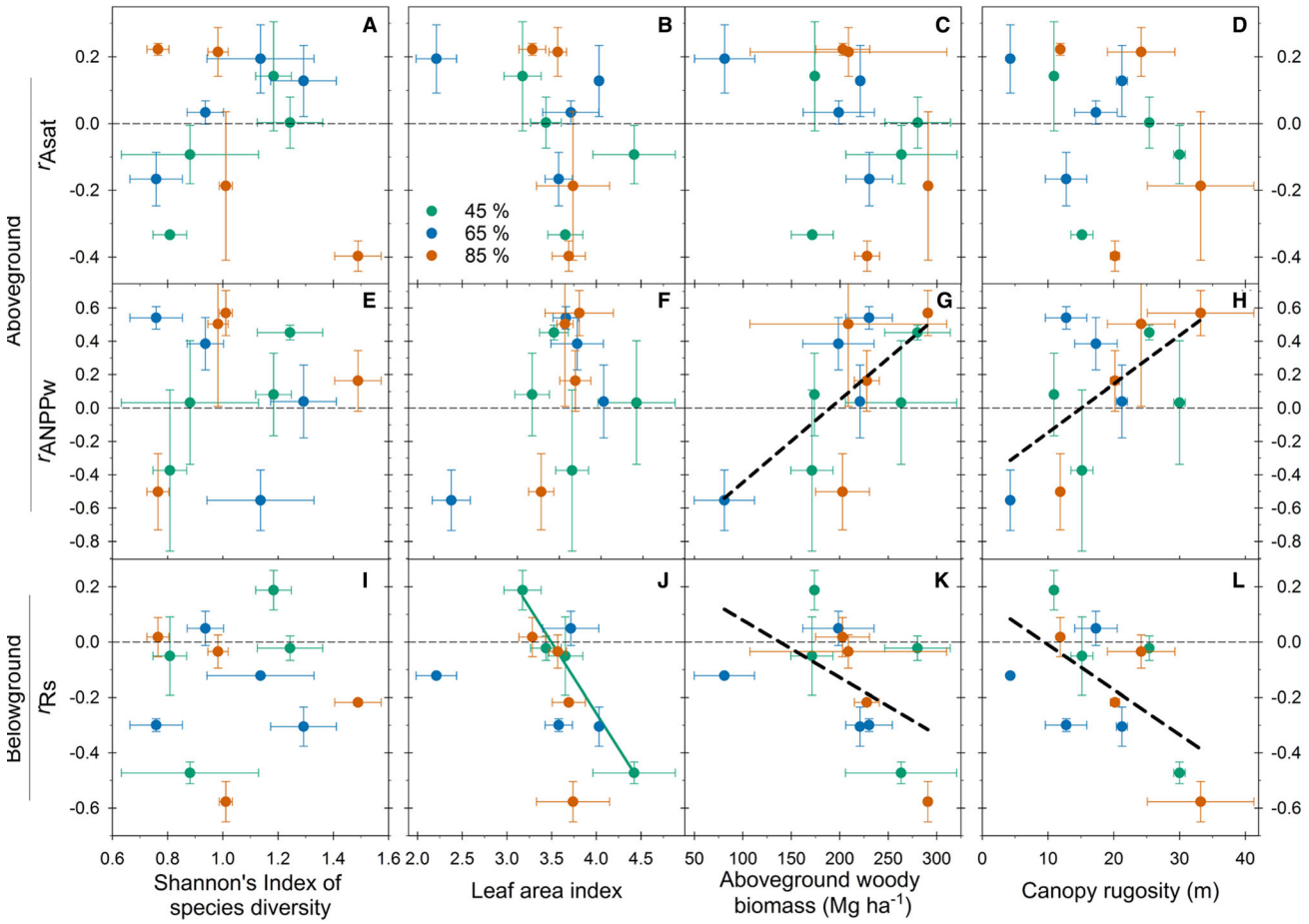

Figure 5. Resistances of subcanopy light-saturated leaf CO_2 assimilation rate ($r_{A_{sat}}$, **A–D**), aboveground wood net primary production (r_{NPP}, **E–H**) and soil respiration (r_{R_s}, **I–L**) in relation to pre-disturbance Shannon's index of diversity, leaf area index, (woody plant) biomass and canopy rugosity. Dashed black lines indicate a common significant relationship among disturbance severities and colored solid lines illustrate significance within a disturbance severity level ($P < 0.1$); lines are omitted when relationships were not significant ($P > 0.1$). Inset legend indicates the percentage of LAI-weighted biomass disturbed via stem girdling. Statistical parameters, including P, goodness of fit (r^2), and linear model coefficients, are in Table S3.

the plot level, we observed significant LAI increases and decreases in separate control plots, and significant decreases averaging 19% in two of four plots at the 85% disturbance severity level (Table S4). These results suggest changes in LAI are underway, but that upper canopy cover was relatively unaffected by phloem disruption in the first growing season following disturbance.

Subcanopy A_{sat} values were similar in the control and disturbed treatments, while significant differences among disturbance severities in $ANPP_w$ and R_s emerged in the first year following disturbance (Figure 3), despite minimal changes in LAI. Mean subcanopy A_{sat}, sampled once during the growing season, was about 5 μmol m^{-2} s^{-1} irrespective of disturbance severity, while displaying high plot-to-plot variation from about 3 to 7 μmol m^{-2} s^{-1} (Figure 3A). In contrast, pairwise comparisons indicate that daily $ANPP_w$ was initially higher in the control treatment after stem girdling, but, following a reversal in the latter half of the growing season, aboveground woody biomass production was higher in the 65 and 85% disturbance severity treatments (Figure 3B). Despite differences in late-season daily aboveground wood production, annual $ANPP_w$ was similar among the disturbance severity treatments, averaging 2250 kg C ha^{-1} y^{-1} experiment-wide. Soil respiration diverged among disturbance severities in mid-July, 2 months following stem girdling, and the change in R_s was negatively proportional to the severity of disturbance (Figure 3C). R_s peaked during mid-summer, reaching mean values of 4.5 μmol m^{-2} s^{-1} and 7.3 μmol m^{-2} s^{-1} in the 85% and control distur-

bance severity treatments, respectively, before declining to a common November mean of 1.2 μmol m^{-2} s^{-1}. Significant differences were not observed between top-down and bottom-up disturbance types for A_{sat}, $ANPP_w$ or R_s (data not shown).

Carbon Cycling Resistance

In the first year following phloem disruption, aboveground processes, A_{sat} and $ANPP_w$, exhibited stable resistance as disturbance severity increased, whereas R_s resistance declined. Mean A_{sat} and $ANPP_w$ resistances sustained values close to zero across the range of disturbance severities, pointing to high initial stability in the months that followed phloem disruption. In contrast, R_s resistance significantly declined as disturbance severity increased, becoming negative (that is, < 0) at the highest (85%) disturbance severity level. The type of disturbance did not affect the first-year resistance of C cycling processes.

Within each disturbance treatment category, large interquartile ranges (Figure 4) underscore the high variation in C cycling stability among landscape ecosystems. First-year resistances varied by up to about 270% and included positive and negative values, indicating a wide range of initial functional responses to disturbance among landscape ecosystems.

Vegetation Characteristics and Carbon Cycling Resistance

Prior to phloem-disrupting disturbance, landscape ecosystems varied significantly in woody plant biomass, LAI and canopy rugosity but not species diversity or stem density (Figure 2A; Table 1). As landscape ecosystems varied from lower to higher productivity, significant differences were observed in LAI from 2.9 to 4.1; aboveground woody biomass from 155,900 to 264,600 kg C ha^{-1}; and canopy rugosity from 8.9 to 28.8 m. Most notably, canopy rugosity differed significantly among all landscape ecosystems, highlighting the broad range in structural complexity across disturbance treatment replicates. In contrast, Shannon's Index of species diversity averaged 1.02 and stem density (≥ 8 cm DBH) averaged 865 stems ha^{-1}, with neither significantly differing among landscape ecosystems.

Pre-disturbance vegetation characteristics had variable effects on first-year C cycling resistance to disturbance (Figure 5). Pre-disturbance LAI, biomass and canopy rugosity did not predict A_{sat} resistance. In contrast, greater pre-disturbance aboveground woody biomass and canopy rugosity led to similar significant increases in first-year $ANPP_w$ resistance for all disturbance severities. R_s resistance trended in the opposite direction, with greater pre-disturbance LAI associated with significantly declining resistance at the 45% disturbance severity level, and higher aboveground woody biomass and canopy rugosity leading to similar significant declines in R_s resistance among disturbance severities. Among the four pre-disturbance vegetation characteristics examined, only species diversity failed to predict the first-year A_{sat}, $ANPP_w$, or R_s resistance of one or more disturbance severities.

DISCUSSION

Our analysis of first-year above- and belowground C cycling responses to disturbance yielded three primary findings. First, we found that C cycling resistance spanned positive and negative values at the plot scale, suggesting that declines and increases in functioning occurred immediately following disturbance at a small (0.5 ha) spatial scale. Secondly, as disturbance severity increased, we observed sustained resistance of aboveground C cycling processes, A_{sat} and $ANPP_w$, and, conversely, a reduction in R_s resistance in the first year that followed phloem-disruption. Lastly, our results illustrate that $ANPP_w$ and R_s resistances were predicted by one or more pre-disturbance vegetation characteristics—namely, canopy rugosity and biomass—highlighting the important but variable role of vegetation structure in supporting initial C cycling responses to disturbance.

Several vegetation characteristics predicted C cycling responses to disturbance, but the sign, strength and consistency of these relationships varied among C cycling processes. We found that pre-disturbance aboveground woody biomass and canopy rugosity were positively related to $ANPP_w$ resistance and negatively correlated with R_s resistance, irrespective of disturbance severity. Contrasting (positive and negative) relationships between $ANPP_w$ and R_s resistance likely reflect immediate—but opposite—shifts in above- and belowground C allocation following phloem girdling (Regier and others 2010). The elimination of photosynthate transport to roots may rapidly reduce root metabolism and, consequently, soil respiration (Bond-Lamberty and others 2011), whereas a concurrent accumulation of carbohydrates above the severed phloem may increase aboveground growth (Högberg and others 2001).

Subcanopy A_{sat} was not correlated with pre-disturbance vegetation characteristics, possibly because the changes in LAI in the months that followed stem girdling disturbance were not sufficient to alter the subcanopy light environment and, consequently, leaf physiology (Stuart-Haentjens and others 2015).

Pre-disturbance structural complexity and biomass may strongly predict increasing $ANPP_w$ and, conversely, declining R_s resistance because complex forests with more biomass have an abundance of heterogeneously distributed live vegetation to compensate for declining individuals and, because they possess larger root systems, may exhibit greater reductions in soil respiration following disturbance (Högberg and others 2009). However, several environmental and ecological variables that influence both production and soil respiration covary with aboveground woody biomass and canopy structural complexity, and their individual influences are not easily disentangled (Chen and others 2011). Similar studies of first-year C cycling resistance in relation to pre-disturbance biomass and other vegetation characteristics are lacking for comparison, but longer-term (that is, temporal) stability may be greater in forests with higher diversity and structural complexity (Fotis and others 2018; Jactel and others 2017; Jucker and others 2014; Musavi and others 2017). Although we did not observe an effect of species diversity on C cycling resistance, relatively low diversity within and among landscape ecosystems at our site may limit the influence of this property on functioning, exposing the limitation of diversity as a predictor of stability in low diversity ecosystems (Wales and others 2020).

We found that aboveground C uptake-related processes exhibited high first-year resistance to disturbance, whereas soil respiration rapidly declined as disturbance severity increased. Although not a complete picture of the ecosystem C cycle, these findings are consistent with the overall C balance being maintained in this early stage of the disturbance and recovery cycle. Such high initial resistance of C uptake processes is in agreement with longer-term observations of NPP and net ecosystem production following disturbance at our site (Gough and others 2013; Stuart-Haentjens and others 2015), although we acknowledge the dynamic behavior of C fluxes following disturbance and the uncertainty of future change (Amiro and others 2010).

Aboveground, C uptake-related processes may have been resistant to disturbance in the first year because stem girdling, like boring insects, abruptly eliminates the transport of carbohydrates to the roots but may not immediately compromise leaf physiology (Dietze and Matthes 2014). Consistent with sustained leaf physiological functioning, we observed no treatment level changes in LAI during the first growing season following disturbance and declines during the leaf-on period of less than 20% occurred in a minority ($n = 3$) of plots. The retention of LAI and high above-ground C cycling resistance that we observed in the first year following phloem disruption may not apply to other disturbance sources, with defoliating insects and severe fire registering more rapid leaf physiological and NPP responses (Amiro and others 2010; Clark and others 2018; Clark and others 2010; Flower and Gonzalez-Meler 2015).

In contrast to aboveground C cycling processes, disturbances that abruptly eliminate non-structural carbohydrate transport to the roots—whether immediately defoliating or not—reduce autotrophic metabolism and, consequently, rapidly affect *in situ* soil respiration (Högberg and others 2001; Levy-Varon and others 2012; Nave and others 2011). Despite signs of first-year stability, we anticipate future declines in net C balance as decomposition fueled by an influx of detritus increases, particularly at high disturbance severity levels. An increase in heterotrophic respiration from disturbance-prompted detritus inputs generally lags behind more immediate shifts in autotrophic respiration (Harmon and others 2011; Schmid and others 2016).

We anticipated that vegetation characteristics would be more essential to sustaining functioning at high disturbance severities (Reyer and others 2015; Seidl and others 2016). We did not find support for this hypothesis, however, despite theoretical assumptions that limiting biotic resources become increasingly important to stability as ecosystem degradation increases, consistent with state change theory proposing that ecosystems with few biotic resources are closer to a critical resistance threshold or transition point (Scheffer and Carpenter 2003). Although $ANPP_w$ resistance in the lowest severity treatment was sensitive to pre-disturbance LAI, the effects of aboveground woody biomass and canopy rugosity on $ANPP_w$ and R_s resistance were similar among disturbance severities. This may be a consequence of the restricted range of observed defoliation in the first year following phloem-disruption, despite targeted long-term gross defoliation levels of 45–85%. Our inconclusive results reinforce the call for longitudinal studies that identify the mechanistic underpinnings of temporally dynamic C cycling stability across gradients of disturbance severity.

In this early stage of the disturbance and recovery cycle, the canopy stratum most affected by stem girdling (that is, disturbance type) had no effect on the resistance of C cycling processes. We expected that an abundance of smaller stems with high root/shoot would drive larger declines in soil respiration in the bottom-up treatment, as photosynthate fueling root metabolism declined in response to phloem girdling (Mei and others 2015). Higher root/shoot is associated with elevated soil respiration (Misson and others 2006), but the quantity of belowground biomass may not parallel root metabolic activity (Weemstra and others 2016). We may not have detected a disturbance type effect on C cycling resistances because differences in root/shoot or whole-ecosystem root metabolism between the bottom-up and top-down disturbance types was less than expected in this early post-disturbance stage, when an abundance of stored carbohydrates are available to power root metabolism (Gough and others 2009). Resolving the mechanisms that underlie differences in C cycling responses among disturbance types remains an ecological frontier, one that is essential to forecasting shifts in the C cycle with increasingly varied and novel disturbance regimes (Buma 2015; Dietze and Matthes 2014).

Our results highlight how opposing small-scale responses to disturbance may offset one another, stabilizing landscape-scale C cycling processes. For example, we observed positive and negative $ANPP_w$ resistance values at the plot-scale, suggesting that overyielding in some plots offset compromised growth in others. Landscapes regularly exhibit less functional amplitude than their individual components because offsetting processes at fine (for example, neighborhood, patch or gap) scales stabilize larger-scale functioning (Turner and others 1993). In addition to the magnitude of change, differences among small spatial scales in the timing of functional change may attenuate landscape responses to disturbance (Kashian and others 2006). These results highlight the time and scale dependencies of functional resistance and, more broadly, reinforce that caution is warranted when assuming uniform stability among different ecosystems or inferring large spatial scale stability from individual ecosystem constituents (Turner 2010).

Our findings require contextualization and acknowledgement of our study's limitations. First, as discussed, functional resistance—our focus—is only one of several dimensions of stability (Hillebrand and others 2018). High first-year resistance does not automatically imply long-term C cycling stability or guarantee a return to pre-disturbance functioning (Hillebrand and Kunze 2020). Second, forest C cycling processes are dynamic following disturbance, requiring years to decades to complete a disturbance and recovery cycle (Amiro and others 2010; Hicke and others 2012). The gradual recovery of ''slow-turnover'' ecosystems such as forests highlights the need for long-term observations of functional change alongside investigation of the underlying and equally dynamic mechanisms that lead to the loss and eventual recovery of ecosystem functioning. Indeed, our first-year observations reinforce the dynamic nature of functional change and stability following disturbance and we expect C cycling resistance, along with other stability measures, to change over time. Lastly, although our analysis encompassed major components of the ecosystem C budget for our site (Gough and others 2008), we did not include root or leaf production. In light of changes in above-belowground C allocation stemming from phloem girdling, inclusion of root and leaf production along with the partitioning of autotrophic and heterotrophic respiration is necessary for robust derivation of net C balance. The integration of C flux components and investigation of the full net C balance is a priority for our project moving forward.

CONCLUSIONS

We conclude that first-year changes in forest C cycling can be predicted for some, but not all processes, from pre-disturbance vegetation characteristics. Specifically, our findings suggest that vegetation characteristics such as structural complexity and biomass may aid in forecasting initial C cycling stability following disturbance. Furthermore, our results reinforce recommendations that management for sustained terrestrial C storage amidst rising global disturbance cultivate vegetation characteristics—including high complexity and productivity—that stabilize C uptake and lessen C losses (Birdsey and Pan 2015). Finally, our analysis demonstrates how a standardized expression of resistance can facilitate direct comparisons of C cycling processes following disturbance. Multidimensional stability frameworks, developed and embraced by population and community ecologists, are not widely used by ecosystem ecologists—particularly those studying forests—to assess functional responses to disturbance. Our application of a standardized resistance measure to the analysis of C cycling responses to disturbance highlights how the broader adoption of such an approach by C cycling scientists may enrich comparisons of dis-

turbance sources and severities, ecosystems and functions.

ACKNOWLEDGEMENTS

Our work was funded by the National Science Foundation, Division of Environmental Biology, Award 1655095. We thank the University of Michigan Biological Station for logistical and technical support, and the use of research infrastructure. We appreciate comments supplied by two anonymous reviewers and the Subject Editor, Dr. Seidl.

DATA AND CODE AVAILABILITY

Data used in this analysis are available via the R FoRTE data package: https://fortexperiment.github.io/fortedata/. Derived data products and statistical analysis are available via: https://doi.org/10.5281/zenodo.3779040.

REFERENCES

Amiro BD, Barr AG, Barr JG, Black TA, Bracho R, Brown M, Chen J, Clark KL, Davis KJ, Desai AR and others. 2010. Ecosystem carbon dioxide fluxes after disturbance in forests of North America. Journal of Geophysical Research-Biogeosciences 115:1–13.

Atkins JW, Bohrer G, Fahey RT, Hardiman BS, Morin TH, Stovall AEL, Zimmerman N, Gough CM. 2018a. Quantifying vegetation and canopy structural complexity from terrestrial LiDAR data using the forestr R package. Methods in Ecology and Evolution 9(10):2057–66.

Atkins JW, Fahey RT, Hardiman BH, Gough CM. 2018b. Forest canopy structural complexity and light absorption relationships at the subcontinental scale. Journal of Geophysical Research-Biogeosciences 123(4):1387–405.

Birdsey R, Pan Y. 2015. Trends in management of the world's forests and impacts on carbon stocks. Forest Ecology and Management 355:83–90.

Bond-Lamberty B, Bronson D, Bladyka E, Gower ST. 2011. A comparison of trenched plot techniques for partitioning soil respiration. Soil Biology & Biochemistry 43(10):2108–14.

Borkhuu B, Peckham SD, Ewers BE, Norton U, Pendall E. 2015. Does soil respiration decline following bark beetle induced forest mortality? Evidence from a lodgepole pine forest. Agricultural and Forest Meteorology 214:201–7.

Brockerhoff EG, Barbaro L, Castagneyrol B, Forrester DI, Gardiner B, Gonzalez-Olabarria JR, Lyver PO, Meurisse N, Oxbrough A, Taki H et al. 2017. Forest biodiversity, ecosystem functioning and the provision of ecosystem services. Biodiversity and Conservation 26(13):3005–35.

Buma B. 2015. Disturbance interactions: characterization, prediction, and the potential for cascading effects. Ecosphere 6(4):1–15.

Chen GS, Yang YS, Guo JF, Xie JS, Yang ZJ. 2011. Relationships between carbon allocation and partitioning of soil respiration across world mature forests. Plant Ecology 212(2):195–206.

Clark KL, Renninger HJ, Skowronski N, Gallagher M, Schafer KVR. 2018. Decadal-scale reduction in forest net ecosystem production following insect defoliation contrasts with short-term impacts of prescribed fires. Forests 9(3):1–25.

Clark KL, Skowronski N, Hom J. 2010. Invasive insects impact forest carbon dynamics. Global Change Biology 16(1):88–101.

Dietze MC, Matthes JH. 2014. A general ecophysiological framework for modelling the impact of pests and pathogens on forest ecosystems. Ecology Letters 17(11):1418–26.

Dietze MC, Sala A, Carbone MS, Czimczik CI, Mantooth JA, Richardson AD, Vargas R. 2014. Nonstructural carbon in woody plants. Annual Review of Plant Biology 65(65):667–87.

Fahey RT, Stuart-Haentjens EJ, Gough CM, De La Cruz A, Stockton E, Vogel CS, Curtis PS. 2016. Evaluating forest subcanopy response to moderate severity disturbance and contribution to ecosystem-level productivity and resilience. Forest Ecology and Management 376:135–47.

Flower CE, Gonzalez-Meler MA. 2015. Responses of temperate forest productivity to insect and pathogen disturbances. In: Merchant SS, Ed. Annual review of plant biology, Vol. 66. Annual Reviews: Palo Alto. p 547–69.

Fotis AT, Morin TH, Fahey RT, Hardiman BS, Bohrer G, Curtis PS. 2018. Forest structure in space and time: Biotic and abiotic determinants of canopy complexity and their effects on net primary productivity. Agricultural and Forest Meteorology 250:181–91.

Gough CM, Atkins JW, Fahey RT, Hardiman BS. 2019. High rates of primary production in structurally complex forests. Ecology 100(10).

Gough CM, Flower CE, Vogel CS, Dragoni D, Curtis PS. 2009. Whole-ecosystem labile carbon production in a north temperate deciduous forest. Agricultural and Forest Meteorology 149(9):1531–40.

Gough CM, Hardiman BS, Nave LE, Bohrer G, Maurer KD, Vogel CS, Nadelhoffer KJ, Curtis PS. 2013. Sustained carbon uptake and storage following moderate disturbance in a Great Lakes forest. Ecological Applications 23(5):1202–15.

Gough CM, Vogel CS, Hardiman B, Curtis PS. 2010. Wood net primary production resilience in an unmanaged forest transitioning from early to middle succession. Forest Ecology and Management 260(1):36–41.

Gough CM, Vogel CS, Schmid HP, Su HB, Curtis PS. 2008. Multi-year convergence of biometric and meteorological estimates of forest carbon storage. Agricultural and Forest Meteorology 148(2):158–70.

Hardiman BS, Bohrer G, Gough CM, Vogel CS, Curtis PS. 2011. The role of canopy structural complexity in wood net primary production of a maturing northern deciduous forest. Ecology 92(9):1818–27.

Hardiman BS, Gough CM, Halperin A, Hofmeister KL, Nave LE, Bohrer G, Curtis PS. 2013. Maintaining high rates of carbon storage in old forests: a mechanism linking canopy structure to forest function. Forest Ecology and Management 298:111–19.

Harmon ME, Bond-Lamberty B, Tang JW, Vargas R. 2011. Heterotrophic respiration in disturbed forests: a review with examples from North America. Journal of Geophysical Research-Biogeosciences 116:1–17.

Hicke JA, Allen CD, Desai AR, Dietze MC, Hall RJ, Hogg EH, Kashian DM, Moore D, Raffa KF, Sturrock RN et al. 2012. Effects of biotic disturbances on forest carbon cycling in the United States and Canada. Global Change Biology 18(1):7–34.

Hillebrand H, Kunze C. 2020. Meta-analysis on pulse disturbances reveals differences in functional and compositional recovery across ecosystems. Ecology Letters 23(3):413–585.

Hillebrand H, Langenheder S, Lebret K, Lindstrom E, Ostman O, Striebel M. 2018. Decomposing multiple dimensions of stability in global change experiments. Ecology Letters 21(1):21–30.

Högberg P, Bhupinderpal S, Lofvenius MO, Nordgren A. 2009. Partitioning of soil respiration into its autotrophic and heterotrophic components by means of tree-girdling in old boreal spruce forest. Forest Ecology and Management 257(8):1764–7.

Högberg P, Nordgren A, Buchmann N, Taylor AFS, Ekblad A, Hogberg MN, Nyberg G, Ottosson-Lofvenius M, Read DJ. 2001. Large-scale forest girdling shows that current photosynthesis drives soil respiration. Nature 411(6839):789–92.

Jactel H, Bauhus J, Boberg J, Bonal D, Castagneyrol B, Gardiner B, Gonzalez-Olabarria JR, Koricheva J, Meurisse N, Brockerhoff EG. 2017. Tree diversity drives forest stand resistance to natural disturbances. Current Forestry Reports 3(3):223–43.

Johnstone JF, Allen CD, Franklin JF, Frelich LE, Harvey BJ, Higuera PE, Mack MC, Meentemeyer RK, Metz MR, Perry GLW et al. 2016. Changing disturbance regimes, ecological memory, and forest resilience. Frontiers in Ecology and the Environment 14(7):369–78.

Jucker T, Bouriaud O, Avacaritei D, Coomes DA. 2014. Stabilizing effects of diversity on aboveground wood production in forest ecosystems: linking patterns and processes. Ecology Letters 17(12):1560–9.

Kashian DM, Romme WH, Tinker DB, Turner MG, Ryan MG. 2006. Carbon storage on landscapes with stand-replacing fires. Bioscience 56(7):598–606.

Koontz MJ, North MP, Werner CM, Fick SE, Latimer AM. 2020. Local forest structure variability increases resilience to wildfire in dry western U.S. coniferous forests. Ecology Letters 23:483–494.

Lapin M, Barnes BV. 1995. Using the landscape ecosystem approach to assess species and ecosystem diversity. Conservation Biology 9(5):1148–58.

Legendre P, Oksanen J, ter Braak CJF. 2011. Testing the significance of canonical axes in redundancy analysis. Methods in Ecology and Evolution 2(3):269–77.

Levy-Varon JH, Schuster WSF, Griffin KL. 2012. The autotrophic contribution to soil respiration in a northern temperate deciduous forest and its response to stand disturbance. Oecologia 169(1):211–20.

Liu YL, Kumar M, Katul GG, Porporato A. 2019. Reduced resilience as an early warning signal of forest mortality. Nature Climate Change 9(11):880.

Mei L, Xiong YM, Gu JC, Wang ZQ, Guo DL. 2015. Whole-tree dynamics of non-structural carbohydrate and nitrogen pools across different seasons and in response to girdling in two temperate trees. Oecologia 177(2):333–44.

Misson L, Gershenson A, Tang JW, McKay M, Cheng WX, Goldstein A. 2006. Influences of canopy photosynthesis and summer rain pulses on root dynamics and soil respiration in a young ponderosa pine forest. Tree Physiology 26(7):833–44.

Musavi T, Migliavacca M, Reichstein M, Kattge J, Wirth C, Black TA, Janssens I, Knohl A, Loustau D, Roupsard O and others . 2017. Stand age and species richness dampen interannual variation of ecosystem-level photosynthetic capacity. Nature Ecology & Evolution 1(2):1–6.

Nave LE, Gough CM, Maurer KD, Bohrer G, Hardiman BS, Le Moine J, Munoz AB, Nadelhoffer KJ, Sparks JP, Strahm BD and others . 2011. Disturbance and the resilience of coupled carbon and nitrogen cycling in a north temperate forest. Journal of Geophysical Research-Biogeosciences 116:1–14.

Pearsall DR, Barnes BV, Zogg GR, Lapin M, Ring RR. 1995. Landscape ecosystems of the University of Michigan Biological Station. School of Natural Resources & Environment. University of Michigan, Ann Arbor, MI, p. 66.

Pedro MS, Rammer W, Seidl R. 2015. Tree species diversity mitigates disturbance impacts on the forest carbon cycle. Oecologia 177(3):619–30.

Radchuk V, De Laender F, Cabral JS, Boulangeat I, Crawford M, Bohn F, De Raedt J, Scherer C, Svenning JC, Thonicke K et al. 2019. The dimensionality of stability depends on disturbance type. Ecology Letters 22(4):674–84.

Regier N, Streb S, Zeeman SC, Frey B. 2010. Seasonal changes in starch and sugar content of poplar (*Populus deltoides* x nigra cv. Dorskamp) and the impact of stem girdling on carbohydrate allocation to roots. Tree Physiology 30(8):979–87.

Reyer CPO, Brouwers N, Rammig A, Brook BW, Epila J, Grant RF, Holmgren M, Langerwisch F, Leuzinger S, Lucht W et al. 2015. Forest resilience and tipping points at different spatio-temporal scales: approaches and challenges. Journal of Ecology 103(1):5–15.

Scheffer M, Carpenter SR. 2003. Catastrophic regime shifts in ecosystems: linking theory to observation. Trends in Ecology & Evolution 18(12):648–56.

Scheuermann CM, Nave LE, Fahey RT, Nadelhoffer KJ, Gough CM. 2018. Effects of canopy structure and species diversity on primary production in upper Great Lakes forests. Oecologia 188(2):405–15.

Schmid AV, Vogel CS, Liebman E, Curtis PS, Gough CM. 2016. Coarse woody debris and the carbon balance of a moderately disturbed forest. Forest Ecology and Management 361:38–45.

Seidl R, Spies TA, Peterson DL, Stephens SL, Hicke JA. 2016. Searching for resilience: addressing the impacts of changing disturbance regimes on forest ecosystem services. Journal of Applied Ecology 53(1):120–9.

Stuart-Haentjens E, De Boeck HJ, Lemoine NP, Mand P, Kroel-Dulay G, Schmidt IK, Jentsch A, Stampfli A, Anderegg WL, Bahn M et al. 2018. Mean annual precipitation predicts primary production resistance and resilience to extreme drought. Science of the Total Environment 636:360–6.

Stuart-Haentjens EJ, Curtis PS, Fahey RT, Vogel CS, Gough CM. 2015. Net primary production of a temperate deciduous forest exhibits a threshold response to increasing disturbance severity. Ecology 96(9):2478–87.

Turner MG. 2010. Disturbance and landscape dynamics in a changing world. Ecology 91(10):2833–49.

Turner MG, Romme WH, Gardner RH, Oneill RV, Kratz TK. 1993. A revised concept of landscape equilibrium—disturbance and stability on scaled landscapes. Landscape Ecology 8(3):213–27.

Wales SB, Kreider MR, Atkins J, Hulshof CM, Fahey RT, Nave LE, Nadelhoffer KJ, Gough CM. 2020. Stand age, disturbance history and the temporal stability of forest production. Forest Ecology and Management 460:117865, 1-9.

Weemstra M, Mommer L, Visser EJW, van Ruijven J, Kuyper TW, Mohren GMJ, Sterck FJ. 2016. Towards a multidimensional root trait framework: a tree root review. New Phytologist 211(4):1159–69.